



Published in final edited form as:

*J Am Chem Soc.* 2010 January 27; 132(3): 1018–1022. doi:10.1021/ja9061272.

## Array Based Sensing of Normal, Cancerous and Metastatic Cells using Conjugated Fluorescent Polymers

Avinash Bajaj<sup>§</sup>, Oscar R. Miranda<sup>§</sup>, Ronnie Phillips<sup>#</sup>, Ik-Bum Kim<sup>#</sup>, D. Joseph Jerry<sup>‡</sup>, Uwe H. F. Bunz<sup>#</sup>, and Vincent M. Rotello<sup>§</sup>

<sup>§</sup>Department of Chemistry University of Massachusetts, 710 North Pleasant Street, Amherst, Massachusetts 01003

<sup>‡</sup>Department of Veterinary and Animal Science, University of Massachusetts, 710 North Pleasant Street, Amherst, Massachusetts 01003

<sup>#</sup>Department of School of Chemistry and Biochemistry, Georgia Institute of Technology, 901 Atlantic Drive, Atlanta, Georgia 30332

### Abstract

A family of conjugated fluorescent polymers was used to create an array for cell sensing. Fluorescent conjugated polymers with pendant charged residues provided multivalent interactions with cell membranes, allowing the detection of subtle differences between different cell types on the basis of cell surface characteristics. Highly reproducible characteristic patterns were obtained from different cell types as well as from isogenic cell lines, enabling the identification of cell type as well differentiating between normal, cancerous and metastatic isogenic cell types with high accuracy.

### Introduction

The multivalent capabilities and sensitivity of conjugated polymers to minor conformational or environmental changes makes them ideal candidates for biosensing applications.<sup>1,2</sup> The optical properties of these materials, e.g. i.e. absorption (color) and emission (glow) change significantly in response to even subtle changes in their surroundings. Unlike small molecule fluorophores, conjugated polymers feature a molecular wire effect and polyvalent modes of interactions that can enhance signal generation.<sup>1,2</sup> Moreover, conjugated polymer chains with multiple recognition elements can bind to one analyte molecule, thereby increasing both the binding efficiency and recognition selectivity for specific analytes.<sup>3</sup>

The favorable properties of conjugated polymers have facilitated their applications in biosensing and bioimaging. As an example, the heparin-like properties of a highly negatively charged PPE were shown by staining of hamster fibroblast cells, where PPE binds selectively to fibronectin due to significant electrostatic interactions.<sup>4</sup> Recent studies on cell labeling using polymers<sup>5,6</sup> suggest that conjugated polymers could provide an effective platform for cell sensing, including the detection of cancer cells.

Existing methods for cancer cell detection are in general based on antibody array<sup>7,8</sup> and DNA microarray<sup>9</sup> techniques, and rely on variations in intra- and extracellular protein biomarkers and mutations in genome, respectively. While antibody-based arrays have been quite successful

rotello@chem.umass.edu; uwe.bunz@chemistry.gatech.edu.

**Supporting Information Available.** Complete Ref. <sup>10</sup>, fluorescence titration and unknown samples data. This information is available free of charge via the Internet at <http://pubs.acs.org/>.

in early detection of cancers, they require the availability of specific markers for different cancers, a situation that is not the case with many cancers.<sup>10</sup> There is therefore a need for the development of new biosensor strategies for the detection of cancer cells that can distinguish between cell lines based on more subtle differences.

Chemical nose-based sensor array approaches<sup>11</sup> that exploit differential receptor-analyte binding interactions provide an alternative to lock-and-key approaches that use specific recognition processes. “Electronic noses/tongues” have been employed for a wide variety of analytes, including metal ions,<sup>12</sup> volatile agents,<sup>13</sup> aromatic amines,<sup>14</sup> amino acids,<sup>15</sup> carbohydrates<sup>16</sup> and proteins.<sup>17</sup> While array approaches are quite useful for detection of specific analytes, the sensitivity of these systems to subtle changes in analyte ratios makes them particularly promising for cell sensing applications, as demonstrated by the use of nanoparticle-polymer systems to identify bacteria<sup>18</sup> and mammalian cell types.<sup>19</sup> In this contribution, we exploit the environmentally responsive fluorescence of poly(*paraphenyleneethynylene*)s (PPE) to provide an array-based sensing system (Figure 1) that can differentiate between cell types as well as discern cancerous from non-cancerous mammalian cells. In our approach, we use a differential affinity-based approach as opposed to specific biomarker recognition. The major advantage of this approach is that we do not require knowledge of specific ligands or receptors to differentiate between cell types and states.

## Experimental Section

### Materials and Methods

Polymers **P1-P8** were synthesized as reported previously.<sup>20</sup> The NT2 cell line was obtained from Prof. R. Thomas Zoeller (Biology Department, University of Massachusetts at Amherst, USA). All the cells were grown in DMEM media supplemented with 10% FBS and 1% antibiotics in T75 flasks at 37 °C in a humidified atmosphere containing 5% CO<sub>2</sub>. Cells were regularly passaged by trypsinization with 0.1% trypsin (EDTA 0.02%, dextrose 0.05%, and trypsin 0.1%) in PBS (pH 7.2).

### Cell sensing studies

Cells grown in T75 flasks were washed with DPBS buffer, trypsinized with 1X trypsin and collected in the DMEM media. Cells were spun down, re-suspended in DMEM media (without serum proteins/antibiotics) and counted using hemocytometer. The polymers were dissolved in DPBS buffer (1 ×) to make 100 nM of stock solutions on the basis of their molecular weights. 200 μL of each polymer solution in DPBS was loaded into a well on a 96-well plate (300 μL Whatman<sup>R</sup>) and the fluorescence intensity values at 465 nm was recorded on a Molecular Devices SpectraMax M5 microplate reader with excitation at 430 nm. 10 μL of cell suspension (5,000 cells) was added to each well. The fluorescence intensity values at 465 nm were recorded again. The ratio of the final response to initial fluorescence response before and after addition of cells was treated as the fluorescence response. This process was repeated firstly for four different cancer cell types to generate six replicates of each. We have tested 4 cell types against the eight-polymer array (**P1-P8**) six times, to generate training data matrix of 8 polymers × 4 cell types × 6 replicates. Similarly, a training matrix of 8 polymers × 3 cell types × 6 replicates was generated for three Isogenic cell types. We have used the same volume and concentration of DMEM media for all cell type experiments under identical conditions. Therefore the changes due to DMEM media alone would be same for all the experiments.

### LDA analysis

The raw data matrix was processed using classical linear discriminant analysis (LDA) in SYSTAT (version 11.0).<sup>21,22</sup> In LDA, all variables were used in the model (complete mode) and the tolerance was set as 0.001. The raw fluorescence response patterns were transformed

to canonical patterns where the ratio of between-class variance to the within-class variance was maximized according to the pre-assigned grouping. In a blind experiment, the rates of fluorescence patterns of new case were first converted to canonical scores using discriminate functions established on training samples. Mahalanobis distance<sup>23,24</sup> is the distance of a case to the centroid of a group in a multidimensional space and was calculated for the new case to the centroid of respective groups (normal or cancerous or metastatic cells) of training samples. The new case was assigned to the group with shortest Mahalanobis distance. This processing protocol was performed on the SYSTAT 11 program, allowing the assignment of cells to specific groups.

## Results and Discussion

As a starting point for our studies we have chosen eight conjugated fluorescent polymers (Figure 2) based on a common PPE backbone. These PPEs are water soluble, fluorescent and structurally diverse, possessing various charge characteristics and differing degrees of polymerization. Our hypothesis was that these characteristics should provide these polymers with selective binding properties, and hence differential interactions with different cell surfaces. (Figure 1) These differential interactions involve the electrostatic interactions between the cationic/anionic polymers and cell surface functionality, e.g. lipids, proteins and polysaccharides. These interactions lead to different aggregation behaviors of polymers on the cell surfaces resulting in variation of the polymer fluorescence that can be analyzed by LDA analysis to discriminate different cell types and states.

We have selected four different human cancerous cell lines and three isogenic cells lines. (Table 1) for our studies. Each of these cell types has a different function that would be expected to be manifested in surface functionality in practice. The isogenic breast cell lines provide a particularly valid testbed for our sensor array, as these cells differ only in cell state, providing a model for detection of cancer in clinical settings.

In practice, we first titrated the polymers with different concentrations of cell suspensions to determine the sensitivity of the array. The fluorescence titration studies showed the required sensitivity using  $5 \times 10^3$  cells (**see SI**) so that final cell concentration of cells would be  $5 \times 10^3$  cells/210  $\mu$ L. In all the further experiments, this concentration of cells was used. The fluorescence of the PPE solution (100 nM, on the basis of number-average molecular weight) in phosphate buffered saline (PBS) was recorded. Then  $5 \times 10^3$  cells in 10 $\mu$ L of DMEM media were added to the PPE and the mixture was incubated for 30 min and the fluorescence of the polymer recorded again. The experiments were performed with eight polymers in 6-replicates. The fluorescence response patterns were generated from the ratio of final and initial fluorescence of the polymers. The fluorescence intensity of all of the samples decreases upon exposure to the mammalian cells due to polyvalent interactions of polymers with cell surfaces. To sort out the fluorescence responses that provide the discriminating signatures, we classified the fluorescence data set for all the 8 polymers using classical linear discriminant analysis (LDA) using SYSTAT software (version 11). This statistical analysis method is used to recognize the linear combination of features that differentiate two or more classes of objects or events. Stepwise analysis with different polymer set(s) (i.e. jackknifed classification) was used to determine which polymer set could best differentiate between the cells. The *Jackknifed classification matrix* is an attempt to approximate cross-validation. The *Jackknifed classification matrix* use functions computed from all of the data except the case being classified. Figure 3 presents the Jackknifed classification matrix for all different set of cell lines using different combinations of polymers. As demonstrated in Fig. 3, we pick out different combinations logically ruling out the cases that lead to less separation. Then we consider the combinations containing least number of polymers. We observed the maximum differentiation grouping using four common polymers (**P2, P2, P3, P5**) in the present study. Next, we

subjected the data obtained from different cancer cell types and isogenic cell to LDA analysis using these common set of particles to determine the separation within each class (*vide infra*).

Figure 4a presents the fluorescence response of the four cell lines (HeLa, MCF-7, NT2 and HepG2) to polymers **P1**, **P2**, **P3**, and **P5**. The LDA analysis converts the patterns of training matrix (4 polymers  $\times$  4 cell lines  $\times$  6 replicates) to canonical scores. The first three canonical factors contain 96.7, 3.0 and 0.3% of variance as shown in Figure 4b. In this plot, each point represents the response pattern for a single cell type to the polymer sensor array. In the canonical fluorescence response patterns, the different cell types are clustered into four non-overlapping groups (95% level confidence ellipses) (Figure 4b), indicating the ability of this set of polymers to differentiate between the four different cancer cell types using simple polymer array.

These initial results validate our ability to differentiate cell types phenotypically based on their surface properties. A much more challenging goal is to differentiate cells based on cell state, i.e. the differentiation between genetically identical healthy, cancerous, and metastatic cells. To determine the ability of our sensors to detect and identify cancer, we used three cell lines from genetically identical BALB/c mice (Table 1). CDBgeo cells were prepared by retroviral infection with a marker gene encoding the fusion of  $\beta$ -galactosidase and neomycin resistance. These cells exhibit normal outgrowths when transplanted into mammary fat pads. The TD cells were prepared by treating CDBgeo-cells with 10 ng/mL TGF- $\beta$  for 14 days,<sup>25</sup> withdrawal for five passages resulted in a persistent epithelial-to-mesenchymal transformation: tumorigenic growth resulted when transplanted. The V14 cell line was established from a primary mammary tumor arising in BALB/c-Trp53+/- mice.<sup>26</sup> The cells lack p53 protein and form aggressive tumors that are locally invasive in mice. Therefore, CDBgeo and TD cells differ from each other just a single cell-state transformation. As an example, V14 is different from CDBgeo and TD in just lacking the p53 tumor suppressor gene.

The three cell lines (CDBgeo, TD, and V14) were screened with the eight PPEs; the jackknifed analysis (Figure 3b) indicates that optimal differentiation (94%) was achieved using the same four polymers as before, i.e. **P1**, **P2**, **P3** and **P5**. Figure 5a shows the fluorescence patterns obtained from four polymers **P1**, **P2**, **P3** and **P5** upon their incubation with isogenic cell types. These patterns were reproducible and subjected to LDA analysis (Figure 5b) generating the training matrix of 4 polymers  $\times$  3 cell types  $\times$  6 replicates with first two factors of 96.3 and 3.7% of variance respectively with 94% accuracy. Therefore, using this array based approach we can discriminate the subtle changes between different cell states, providing a model for cancer detection in clinical applications.

The robustness of the polymer array system was tested using unknowns generated from the three isogenic cell lines. The fluorescence response patterns generated were subjected to LDA analysis. During LDA, the cell types were classified to the groups generated through the training matrix according to their shortest Mahalanobis distances to respective groups. In these studies we observed 80% accuracy of unknown samples (19 out of 24).

Analysis of the combined results indicates that four polymers (**P1**, **P2**, **P3** and **P5**) out of the original eight can distinguish different mammalian cells effectively. Of the four polymers **P1-4** are cationic and would hence be expected to interact with the negatively charged cell membrane. Significantly, polymer length is important, as **P3** and **P4** have the same structure, but only the longer **P3** was effective at differentiation, suggesting that polyvalency is an important consideration in differentiation. Polymers **P5-8** are anionic in nature, and their interaction with the cells is not clear. It is worth noting, however, that the least charged anionic polymer (**P5**) was most effective at cell differentiation.

## Conclusions

In summary, we have developed a conjugated fluorescent polymer PPE-based sensor array and demonstrated its utility in cell sensing. Using this sensor array, we can distinguish between several cancer cell types as well as between isogenic healthy, cancerous, and metastatic cells that possess the same genetic background. Taken together, these studies provide an effective sensor for differentiating cell types, as well as provide a potential direction in the creation of polymer-based imaging agents and delivery vehicles based on differential cell interactions; and “nose” based polymer sensor arrays are new ways for diagnostic, biophysical and surface science processes involving cell surfaces.

## Supplementary Material

Refer to Web version on PubMed Central for supplementary material.

## Acknowledgments

We thank Professor R. Thomas Zoeller (Biology Department, University of Massachusetts at Amherst, USA) for providing the NT2cell lines. This work was supported by the NSF Center for Hierarchical Manufacturing at the University of Massachusetts (DMI-0531171), NIH Grants GM077173 (VMR), AI073425, CA095164 and CA105452 to DJJ; and Department of Energy Grant DE-FG02-04ER46141 (U.H.F.B., V.M.R.)

## References

1. Thomas SW, Joly GD, Swager TM. *Chem. Rev* 2007;107:1339. [PubMed: 17385926]
2. McQuade DT, Pullen AE, Swager TM. *Chem. Rev* 2000;100:2537. [PubMed: 11749295]
3. a Yang JS, Swager TM. *J. Am. Chem. Soc.* 1998;120:11844. b Zhou Q, Swager TM. *J. Am. Chem. Soc* 1995;117:12593. c Wang DL, Gong X, Heeger PS, Rininsland F, Bazan GC, Heeger AJ. *Proc. Natl. Acad. Sci* 2002;99:49. [PubMed: 11756675] d Kim IB, Erdogan B, Wilson JN, Bunz UHF. *Chem. Eur. J* 2004;10:6247. e Kim IB, Bunz UHF. *J. Am. Chem. Soc* 2006;128:2818. [PubMed: 16506758]
4. Mcrae RL, Phillips RL, Kim IB, Bunz UHF, Fahmi CJ. *J. Am. Chem. Soc* 2008;130:7851. [PubMed: 18507462]
5. Kim IB, Shin H, Garcia AJ, Bunz UHF. *Bioconjugate Chem* 2007;18:815.
6. Moon JH, McDaniel W, MacLean P, Hancock LE. *Angew. Chem. Intl. Ed* 2007;46:8223.
7. Campagnolo C, Meyers KJ, Ryan T, Atkinson RC, Chen YT, Scanlan MJ, Ritter G, Old LJ, Batt CA. *J. Biochem. Biophys. Methods* 2004;61:283. [PubMed: 15571777]
8. Wingren C, Borrebaeck CA. *Curr. Opin. Biotech* 2008;18:55. [PubMed: 18187318]
9. Petty RD, Nicolson MC, Kerr KM, Collie-Duguid E, Murray GI. *Clin. Cancer Res* 2004;10:3237. [PubMed: 15161676]
10. Croswell JM, et al. *Ann. Fam. Med* 2009;7:212. [PubMed: 19433838]
11. a Kim I-B, Han MH, Phillips RL, Samanta B, Rotello VM, Zhang ZJ, Bunz UHF. *Chem. Eur. J* 2009;15:449. b Wang J, Liu B. *Chem. Comm* 2009:2284. [PubMed: 19377660] c Li HP, Bazan GC. *Adv. Mater* 2009;21:964. d Wright AT, Anslyn EV. *Chem. Soc. Rev* 2006;35:14. [PubMed: 16365639]
12. Lee JW, Lee JS, Chang YT. *Angew Chem. Int. Ed* 2006;45:6485.
13. Rakow NA, Suslick KS. *Nature* 2000;406:710. [PubMed: 10963592]
14. Greene NT, Shimizu KD. *J. Am. Chem. Soc* 2005;127:5695. [PubMed: 15826210]
15. Folmer-Andersen JF, Kitamura M, Anslyn EV. *J. Am. Chem. Soc* 2006;128:5652. [PubMed: 16637629]
16. Buryak A, Severin K. *J. Am. Chem. Soc* 2005;127:3700. [PubMed: 15771496]
17. You CC, Miranda OR, Gider B, Ghosh PS, Kim IB, Erdogan B, Krovi SA, Bunz UHF, Rotello VM. *Nat. Nanotechnol* 2007;2:318. [PubMed: 18654291]
18. Phillips RL, Miranda OR, You CC, Rotello VM, Bunz UHF. *Angew Chem. Int. Ed. Engl* 2008;47:2590. [PubMed: 18228547]

19. Bajaj A, Miranda OR, Kim IB, Phillips RL, Jerry DJ, Bunz UHF, Rotello VM. *Proc. Natl. Acad. Sci. U. S. A* 2009;106:10912. [PubMed: 19549846]
20. a Kim I-B, Dunkhorst A, Gilbert J, Bunz UHF. *Macromolecules* 2005;38:4560. b Tan C-Y, Pinto MR, Schanze KS. *Chem. Commun* 2002:446. c Kim I-B, Phillips RL, Bunz UHF. *Macromolecules* 2007;40:5290. d Miranda OR, You C-C, Phillips R, Kim I-K, Ghosh PS, Bunz UHF, Rotello VM. *J. Am. Chem. Soc* 2007;129:9856. [PubMed: 17658813]
21. SYSTAT11.0 (SystatSoftware, Richmond, CA94804, USA, 2004).
22. Jurs PC, Bakken GA, McClelland HE. *Chem. Rev* 2000;100:2649. [PubMed: 11749299]
23. Mahalanobis PC. *Proc. Natl. Inst. Sci. India* 1936;2:49–55.
24. Gnanadesikan R, Kettenring JR. *Biometrics* 1972;28:81.
25. Deugnier MA, Faraldo MM, Teuliere J, Thiery JP, Medina D, Glukhova MA. *Dev. Biol* 2006;293:414. [PubMed: 16545360]
26. Blackburn AC, McLary SC, Naeem R, Luszcz J, Stockton DW, Donehower LA, Mohammed M, Mailhes JB, Soferr T, Naber SP, Otis CN, Jerry DJ. *Cancer Res* 2004;64:5140. [PubMed: 15289317]



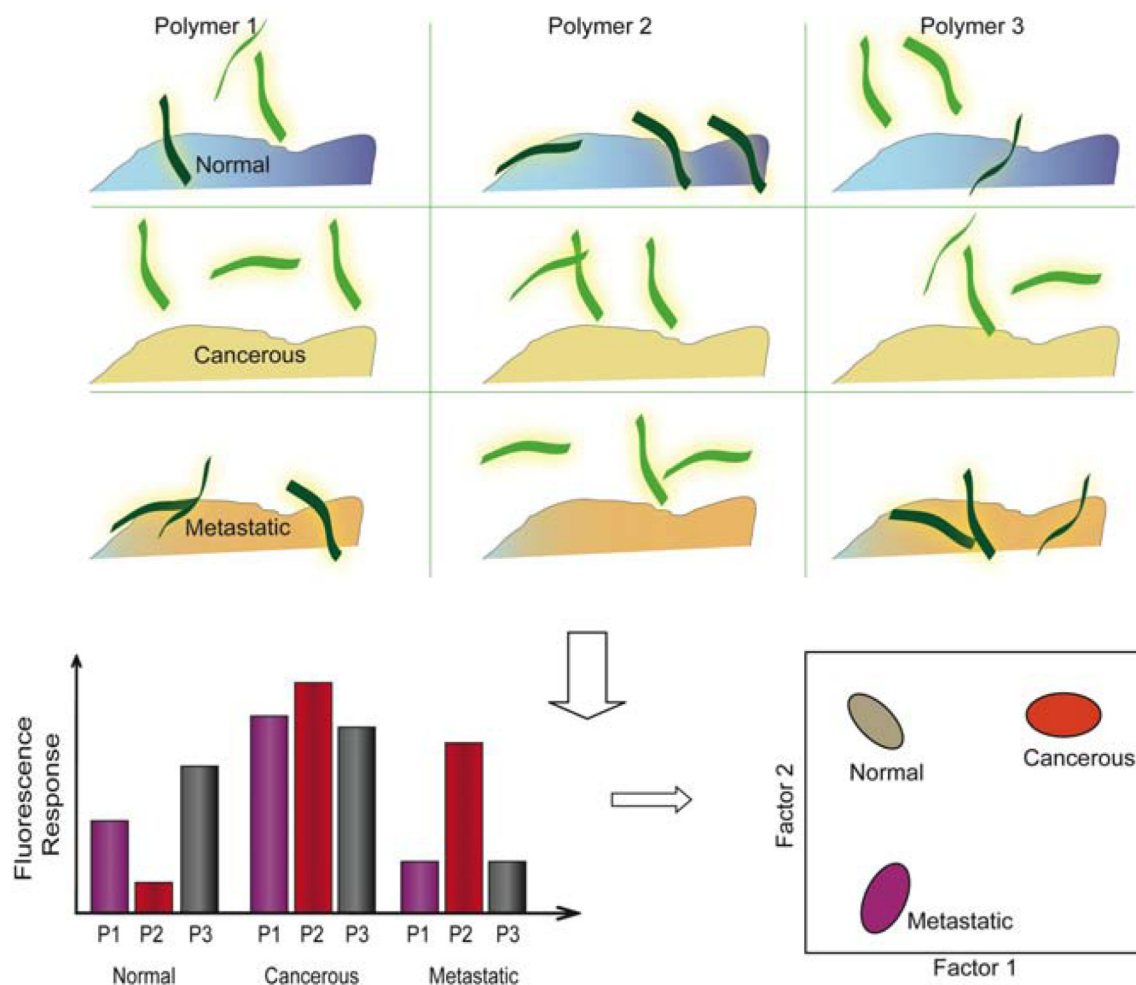
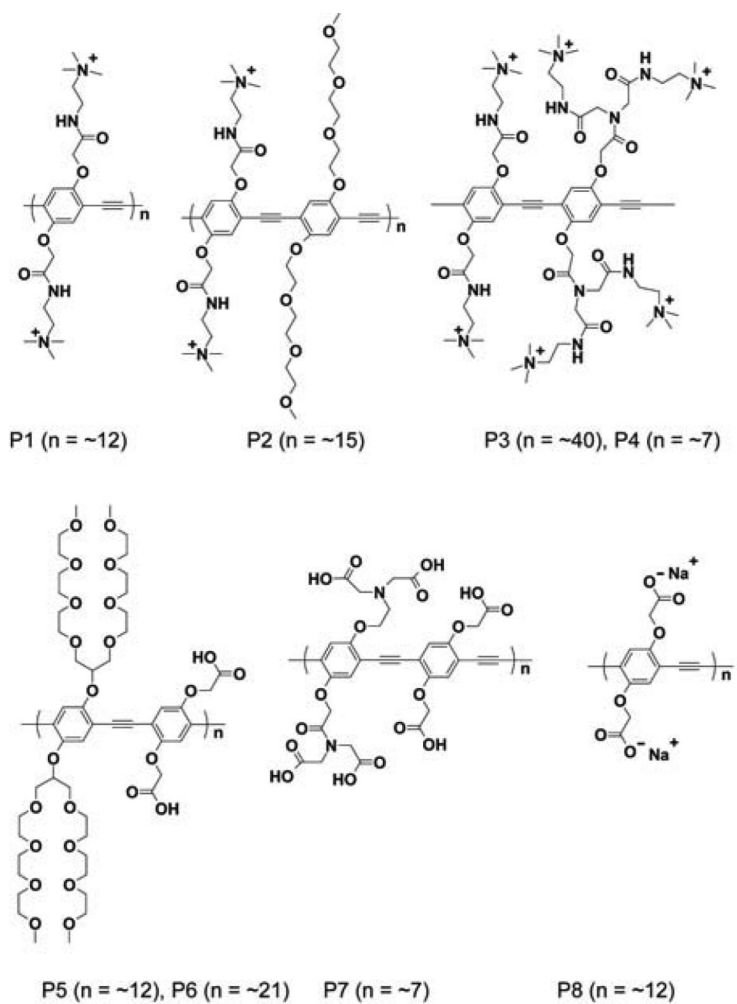


**Figure 1.** Schematic presentation of cell detection assay and interaction between polymers and cell types.



Polymer	$M_n$	$M_w$	PDI	$n$
P-1	5,023	10,246	2.04	12
P-2	10,840	21,029	1.94	15
P-3	49,503	103,956	2.10	40
P-4	8,663	20,271	2.34	7
P-5	14,088	30,092	2.14	12
P-6	25,211	46,313	1.84	21
P-7	6,351	14,887	2.34	7
P-8	3,500	6,600	1.88	12

**Figure 2.** Molecular structures of the fluorescent polymers used in this study.<sup>20</sup>



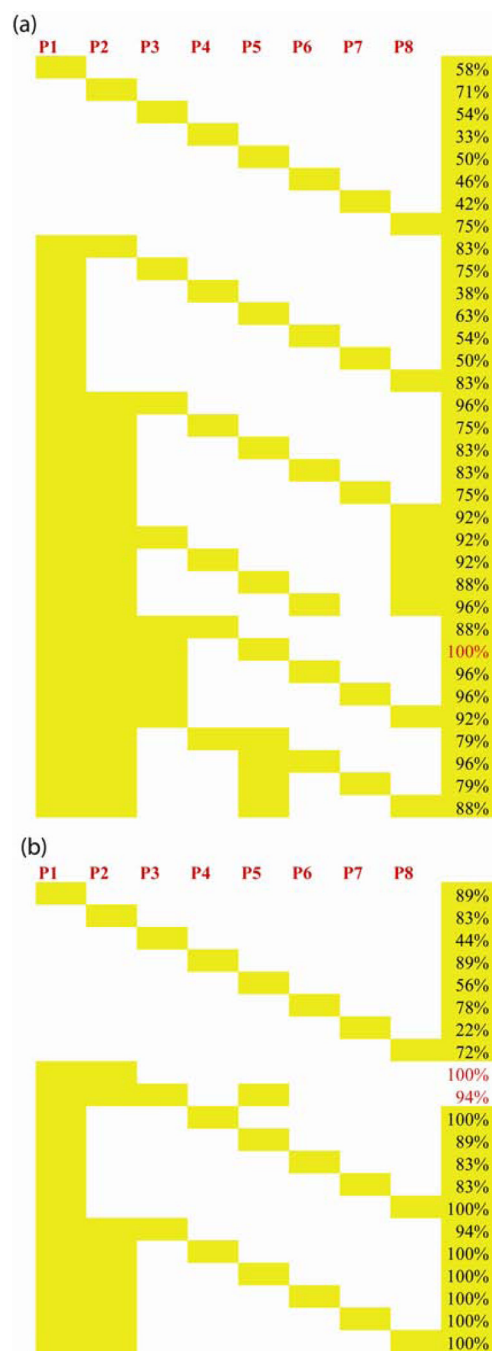


**Figure 3.** Jackknifed classification matrix obtained through LDA analysis for eight polymers for (a) four cell lines HeLa, MCF-7, NT2 and HepG2; (b) for three cell lines CDBge, TD and V14.

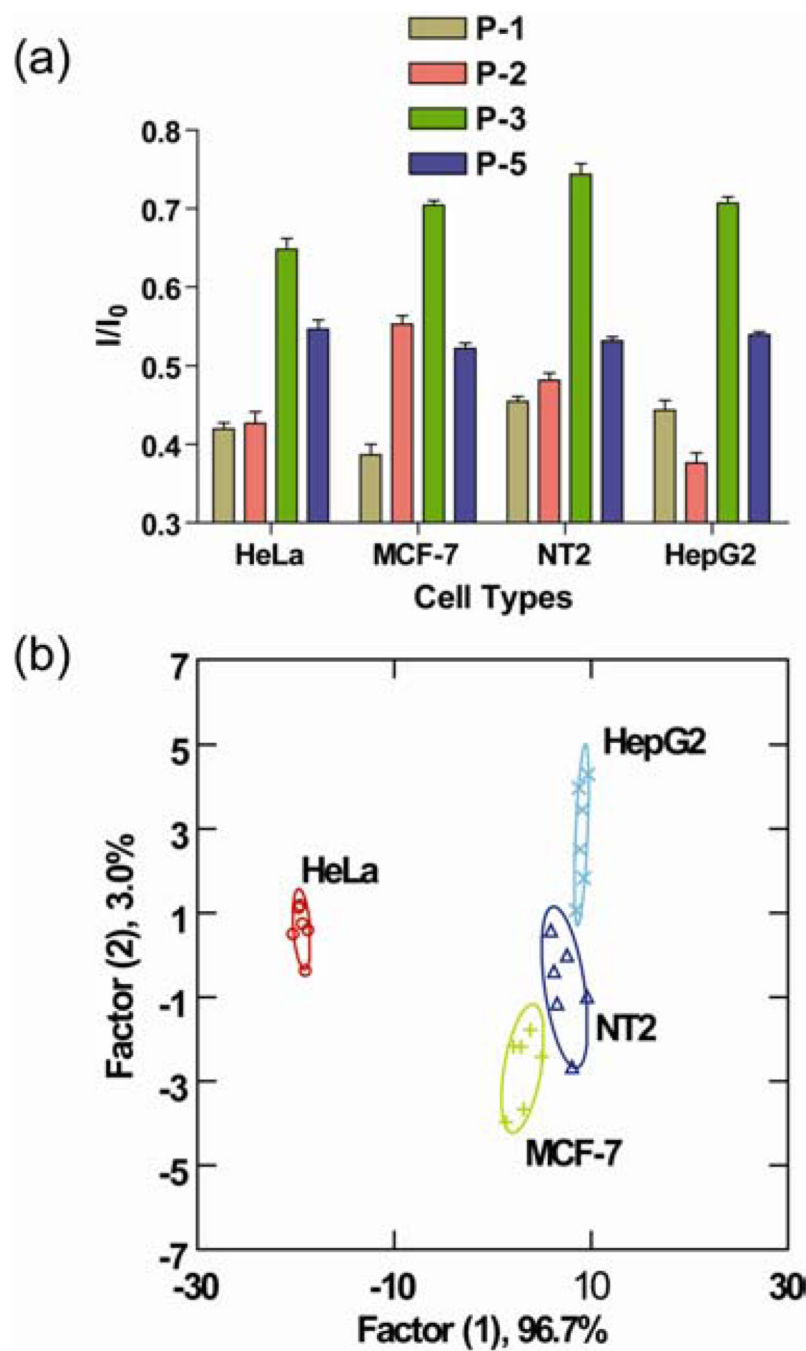


**Figure 4.** (a) Fluorescence responses for four different cancer cell lines HeLa (cervical), MCF7 (breast), HepG2 (liver) and NT2 (testes) using fluorescent polymers. Each value is average of six parallel measurements. (b) Canonical score plot for two factors of simplified fluorescence response patterns obtained with the fluorescent polymer arrays

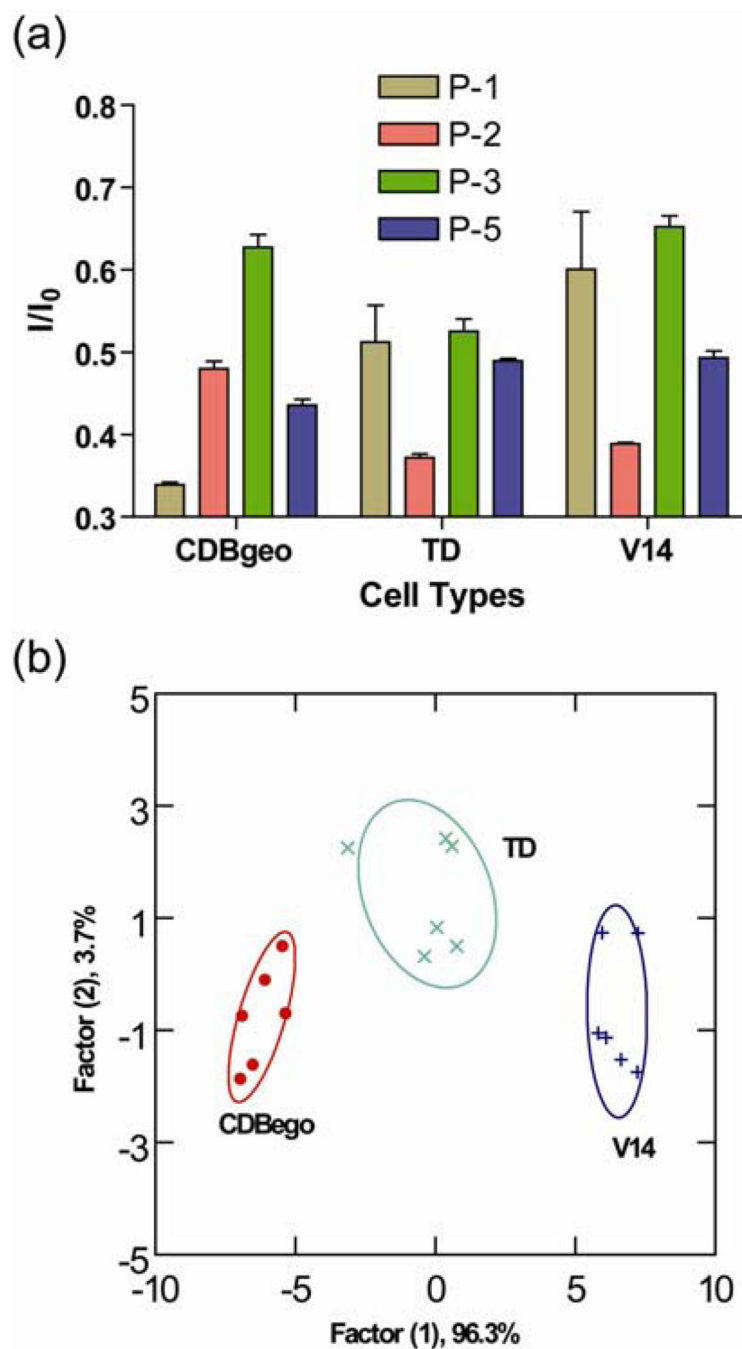


**Figure 5.** (a) Fluorescence responses for three isogenic cell lines CDBgeo, TD cell and V14 using polymer arrays. Each value is average of six parallel measurements. (b) Canonical score plot for first two factors of simplified fluorescence response patterns obtained with polymer arrays against different mammalian cell types. The canonical scores were calculated by LDA for identification of three cell lines.

**Table 1**

Origin and nature of the mammalian cell lines used in this study.

Human cell lines	Cervix	HeLa	Cancerous
	Brest	MCF-7	Cancerous
	Liver	HepG2	Cancerous
	Testis	NT2	Cancerous
Mouse cell lines	BALB/c mice (Breast)	CDBgeo	Normal
			Immortalized
		TD	Cancerous
		V14	Metastatic